ELSEVIER

Marine Geology 249 (2008) 167–183

MARINE GEOLOGY
INTERNATIONAL JOURNAL OF MARINE GEOLOGY, GEOCHEMISTRY AND GEOPHYSICS

www.elsevier.com/locate/margeo

Morphological change and sediment dynamics of the beach step on a macrotidal gravel beach

Martin J. Austin [a,*], Daniel Buscombe [b]

[a] School of Earth, Ocean and Environmental Science, University of Plymouth, Drake Circus, Plymouth, PL4 8AA, UK
[b] School of Geography, University of Plymouth, Drake Circus, Plymouth, PL4 8AA, UK

Received 8 October 2006; received in revised form 2 November 2007; accepted 26 November 2007

Abstract

The morpho-sedimentary evolution of a pure gravel beach step over a tidal cycle is examined during fairweather conditions using detailed measurements of nearshore hydrodynamics, morphological and sedimentary change, and nearshore sediment transport. The characteristics of the beach step are analysed with specific reference to the concurrent dynamics of the beachface, a departure from previous studies which have treated the step as a feature isolated from the nearshore region as a whole. The step and berm are both accretionary features strongly linked to tidal stage, yet their temporal evolution is independent, the relaxation time of the berm being linked to the spring–neap tidal cycle, and that of the more transient step linked to the semi-diurnal tide. Over this time-scale the beachface is a closed sedimentary unit, although the beach step may be differentiated from the beachface using sedimentary moments. Indeed, despite the location of the step in the region of wave breaking, it has relatively stable sedimentology, remaining characteristically coarser and more leptokurtic than the swash zone. Co-spectral analysis between nearshore bed motion and cross-shore current velocity reveals that significant nearshore sediment transport occurs at sub-incident frequencies in response to wave groups. Motion of the nearshore bed is not a linear function of velocity magnitude or direction, so it is likely that there is a role for the various mechanical properties of the bed. Therefore a better description of nearshore sediment transport in the region of the beach step would require instantaneous sediment size information, allowing the use of a time-variant friction factor.

Keywords: beach step; morphodynamics; gravel beach; sediment transport

1. Introduction

Beach steps are morphological features commonly associated with steep, coarse-grained beaches, particularly those composed of gravel. Typically located around the elevation of the mean water level (MWL), the step evolves according to the tidal stage and forms an acute discontinuity in the beach profile at the transition between the breaker and swash regions (e.g. Miller and Zeigler, 1958; Bauer and Allen, 1995; Ivamy and Kench, 2006), and is illustrated in Fig. 1. The sedimentology of the beach step is usually skewed towards the coarsest fraction found on the beachface, the fines having been selectively removed. The importance of the beach step is two-fold. Firstly, due to the abrupt change in water depth, the beach step forms a steep hydrodynamic gradient close to the breakpoint, thereby exerting a control on wave breaking (Hughes and Cowell, 1987). This region is strongly associated with sediment convergence; non-linear shoaling waves transport sediment onshore (Hoefel and Elgar, 2003), whilst the backwash erodes sediment from the lower swash and transports it seawards (Miller and Zeigler, 1958; Strahler, 1966). It could therefore be argued that the step is the coarse beach analogy to the breakpoint bar (Dhyr-Nielsen and Sorensen, 1970; Roelvink and Stive, 1989). Secondly, the beach step plays an important role in the morphological response of reflective (steep) beaches to storms. Beaches typically respond to energetic waves by becoming more dissipative; offshore sediment transport, conductive to bar formation, prevails, and the beach gradient is reduced. However, beaches that display a significant beach step

* Corresponding author.
E-mail addresses: martin.austin@plymouth.ac.uk (M.J. Austin), daniel.buscombe@plymouth.ac.uk (D. Buscombe).

0025-3227/$ - see front matter © 2007 Elsevier B.V. All rights reserved.
doi:10.1016/j.margeo.2007.11.008

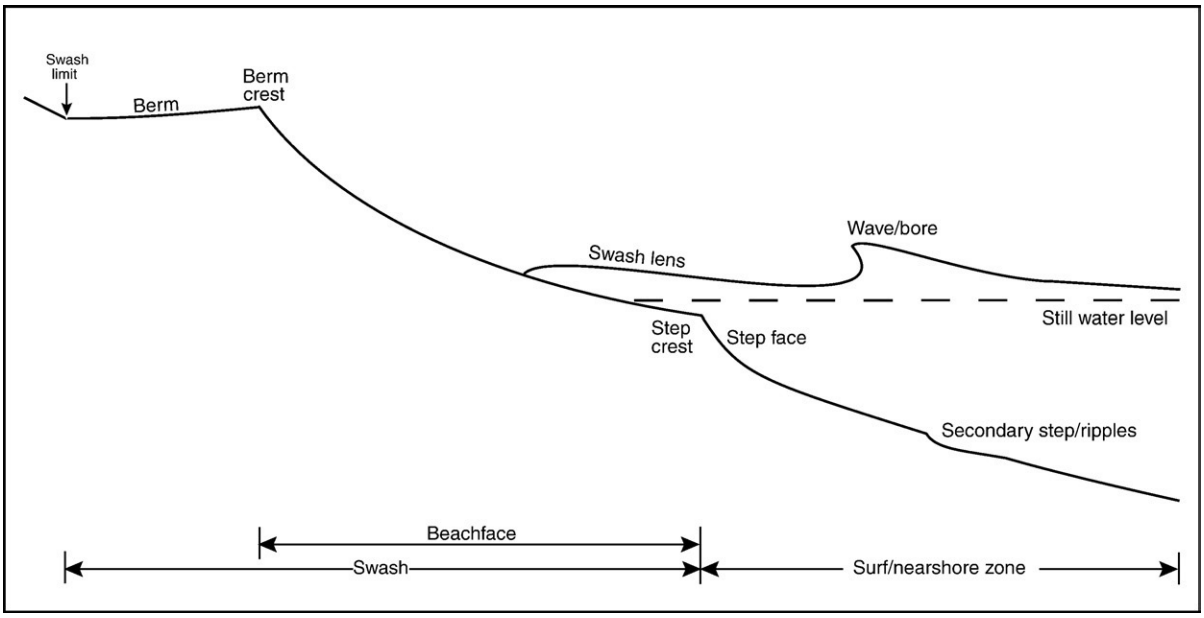

Fig. 1. Generalised schematic diagram of the nearshore profile of a stepped gravel beach indicating the beachface and swash zone morphology, terminology and principal processes found on such a beach.

remain reflective long into storms by increasing the size of the step (Hughes and Cowell, 1987). This forces turbulent wave breaking at the base of the beach and maintains inshore water depth, thereby reducing the sensitivity of the beachface to incident wave energy and preventing the formation of a wide surf zone (Hughes and Cowell, 1987; Austin and Masselink, 2006).

The formation of the beach step has provided an interesting problem for past researchers, and several theories have arisen which attempt to explain its formation; these can be separated into two groups: (1) those associated with sediment convergence and accretionary evolution; and (2) those linked to the formation of a backwash vortex. Miller and Zeigler (1958) and Strahler (1966) argue that the step is an accretionary feature formed by the convergence of sediment at the foreshore base; the incoming wave deposits sediment at the step upon breaking and the backwash draws sediment down-slope from the swash. This also accounts for some of the observed coarsening of the sediments at the step, since wave breaking will remove any fines through suspension processes leaving only the coarse fraction.

The alternative explanation for step formation is the backwash vortex (Matsunaga and Honji, 1980, 1983; Takeda and Sunamura, 1983). Under this hypothesis, flow separation during the backwash creates supercritical flow and vortex formation, whereby landwards flow at the base of the step sustains the step face through avalanching. The flow of water up the step face is thought to maintain fine sediments in suspension, which are subsequently removed by wave induced currents, leaving the coarse fraction at the step. Larson and Sunamura (1993) indicated the importance of phase coupling between incident waves and swash motions to backwash vortex formation thereby suggesting a dependance on wave breaker type (e.g. Kemp, 1975; Bauer and Allen, 1995).

While there have been a number of previous studies that examine the beach step, many of them do so in isolation without consideration of the morphodynamics of the beachface as a whole. For example, the formation and/or migration of a beach step suggests considerable sediment transport—but, a parallel process on most coarse-grained beaches, which also transports a large volume of sediment, is berm formation. Berms principally develop due to asymmetric swash processes stranding sediments around the run-up limit (e.g. Duncan, 1964); however, these sediments must be sourced from lower on the beachface. The step may facilitate berm building by pushing sediments onshore over successive tidal cycles with the result that sediments liberated from depths of several metres must pass through the step region to replenish the beachface. Alternatively, if the volume of sediment landward of the step is plentiful, then the berm may be restructured from these existing materials.

The beach step serves as an ideal setting to examine the relationship between morphological and sedimentological variability, which traditionally receives poor coverage in morphodynamic experiments. The relationship between the spatial variation in sediment size and beach slope is well documented, both in the field (e.g. Krumbein, 1938; Davis, 1985; Inman, 1953) and simulated in the laboratory (e.g., Bagnold, 1940; Kamphuis and Moir, 1977). Sediment size has been invoked to partially explain the development of gravel beach features such as the berm (Masselink and Li, 2001; Austin and Masselink, 2006), and cusps (Sherman et al., 1993). The observed persistence of coarse sediments at the step (Miller and Zeigler, 1958; Bauer and Allen, 1995) would also suggest that sediment size has morphodynamic implications in the region of wave breaking. Indeed, previous studies have suggested that sediment size and morphological change have a co-variability which may reinforce individual distinct morphological features, and sediment transport characteristics through those features, through feedback processes (e.g. Sherman et al., 1993; Tolman, 1994; Rubin and Topping, 2001).

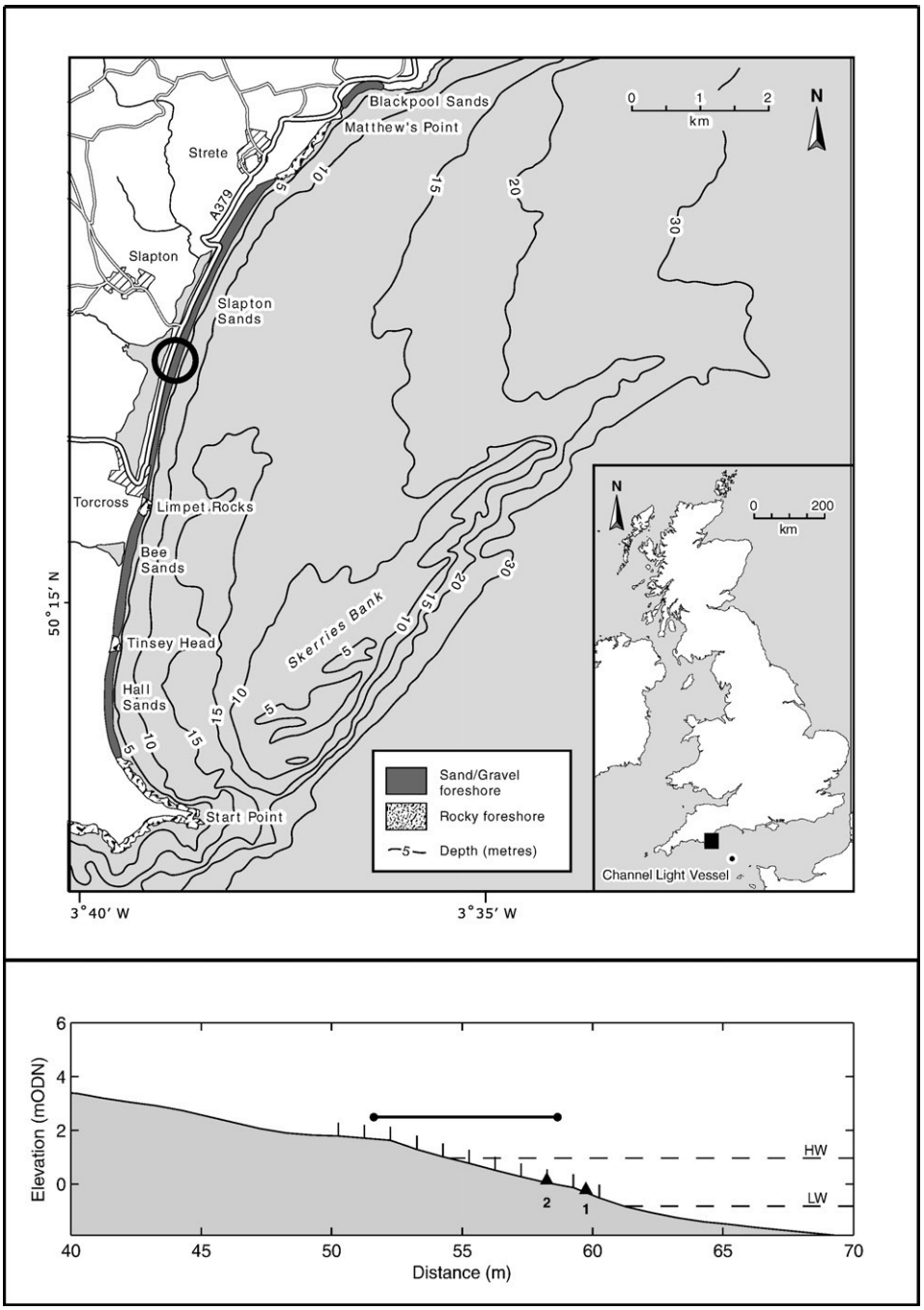

Fig. 2. Location map and beach profile of Slapton Sands. Top—field site (circled); bottom—beach profile with high-tide levels, swash zone, instrument rigs and fibreglass rods. ODN refers to Ordnance Datum Newlyn (approximate mean sea level datum for the UK), HW is the recorded high water level and LW is the recorded low water level. The horizontal line indicates the region of the beach exposed to swash action during the field survey.

Temporal trends in grain-size are often hard to discern. This leads to a conflict between those authors who believe that changes in grain size do not remain correlated through time (e.g. Davis, 1985; Liu and Zarillo, 1989), and those that believe there to be a temporal correlation or 'persistence' in sedimentary data in dynamic sedimentary environments (e.g. Losada et al., 1992). The intermediate case is that morphological change results in a spatial variability in grain-size which displays temporal persistence, but that these are stochastic variations about a 'master' (time-averaged) grain-size distribution (e.g. Guillen and Palanques, 1996; Medina et al., 1994). The latter two cases allow grain size characteristics to have a morphodynamic role in order to partially explain morphological change. In other words, if changes in grain-size and morphology are correlated through time (i.e. they exhibit temporal structure) this would support the suggestion that sediment characteristics may reinforce morphological change (Buscombe and Masselink, 2006).

A dominant influence on the morphodynamics of macrotidal beaches is the tidal state. Variations in water depth result in the horizontal translation of the swash, breaker and shoaling wave

zones across the nearshore in phase with the tide. If it is assumed that the step is maintained roughly at the breakpoint, it should be expected that as the breakpoint migrates with the tide the step should migrate similarly (Bauer and Allen, 1995). However, the above presupposes that the step has a very short relaxation time when it is well acknowledged that there is frequently a significant lag between geomorphic process and resultant morphological change. For example in a nearshore context, Austin et al. (2007) recently showed that ebb tide adjustments to wave ripples on a sandy beach significantly lagged the falling tidal level. Thus there exists the possibility that although the morpho-sedimentary dynamics of the step are likely to be influenced by the tidal state, relaxation times are also likely to be important.

The principal aim of this paper is to describe the morpho-sedimentary evolution of the beach step over a tidal cycle on a macrotidal gravel beach, and investigate whether the morphological response can be traced through temporal and spatial variations in the hydrodynamics, sediment transport and sediment characteristics. Specifically, we test if the step and berm are co-evolutionary and whether periods of morphological change and sediment transport correlate to changes in the hydrodynamic forcing. First, we investigate the hydrodynamics during the field survey followed by an examination of the morphological and sedimentological changes to the beachface and finally an analysis of sediment transport across the foreshore.

2. Field site and methodology

2.1. Location

As part of ongoing field monitoring at Slapton Sands, Devon, UK (2003-date), a field experiment focusing on the beachface region was carried out during September 2005. Slapton Sands is a 4-km long gravel barrier with a width of 100–140 m and a crest elevation of 6–7 m above Ordnance Datum Newlyn (ODN, ~0.2 m above mean sea level). Slapton is aligned in a roughly north–south direction and is backed by a shallow freshwater lagoon (Slapton Ley). The barrier is protected from Atlantic swell propagating up the English Channel by its alignment, the Skerries Bank, and Start Point (Fig. 2). The most energetic wave conditions are due to wind waves from the northeast. The tidal regime is semi-diurnal with spring and neap ranges of 4.3 m and 1.5 m, respectively. As a large gravel barrier, Slapton is unusually fine and well-sorted, possibly because, over long timescales of the order decades–centuries, it is considered a closed sedimentary system (Hails, 1975), with no significant inputs or outputs of sediments into the system. The modern sediments are therefore relict, and have been reworked by wave action for at least 3000 yr (Morey, 1976), making them small, and well rounded. More poorly sorted and irregularly shaped sediments have been found at depth in Start Bay (Hails, 1975).

2.2. Instrumentation

During the field survey two instruments rigs were deployed in a cross-shore transect across the intertidal beachface (Fig. 2). Rig 1, consisted of a Druck pressure transducer (PT) and 2-D Valeport miniature discus head current meter (ECM), and measured water depth h and cross-shore u and alongshore v flow velocity 3 cm above the bed around the mid-step position. Rig 2 was located at the base of the step and measured the velocity 0.1, 0.25 and 0.4 m above the bed with a vertical array of two 3-D Nortek Vector velocimeters (ADV) and an ECM, and water depth with a PT (Fig. 3). An underwater video camera was also mounted at Rig 2, positioned to observe the bed under the current meters, to provide an indication of sediment transport. A further PT (PT3) was mounted on the seabed (at $x=72$ m) below the LW level to monitor the tide and wave conditions input to the beachface. The swash excursion was monitored with a resistance run-up wire, which was calibrated *in-situ*, mounted 2 cm above the bed and extending from the step to landward of the high-tide berm. The PTs, ECMs and run-up wire were centrally logged by a shore-based computer at 16 Hz and the ADVs logged to internal memory at 32 Hz. Images from the underwater camera were digitised directly to a computer at 25 Hz.

The beach profile was surveyed at low tide along a single shore-normal transect using a Trimble electronic total station. Morphological measurements with a higher temporal resolution were carried out during tidal inundation using a rapid profiling method similar to that of Sallenger and Richmond (1984), Nordstrom and Jackson (1990) and Kulkarni et al. (2004). This method is ideally suited to obtaining accurate bed-level data from under water and has been used previously on coarse beaches with consistently good results (Austin and Masselink, 2006); it has an estimated accuracy of ±1 cm. Fibreglass rods (diameter 8 mm) were inserted into the beachface and the exposed length of the rod above the gravel surface was measured at 5-min intervals using a specially-designed ruler. These rapid profile measurements were conducted from the spring high-tide berm to seaward of the step (up to wading water depth).

2.3. Sediment sampling

Two methods of sediment sampling for size were carried out for this study to optimise temporal and spatial resolution within

Fig. 3. Photograph of Rig 2 showing the vertical array of current meters, pressure transducer and underwater video camera prior to deployment.

the experimental set-up. A 10 m transect was established 2 m longshore of the morphological transect, and the sampling frequency at each station was a function of the duration of fluid flow coverage. Therefore the only continuous records of sediment size, sampled every 10-min for the entire 6 h experiment, were at the step and lower swash, where a total of 333 samples were collected. Sub-aqueous sediments from the step face and lower-swash regions were grab-sampled, dried, and sieved at 1/4φ intervals. Intermittently-submerged sediments in the upper swash were photographed every 5-min whilst sub-aerial, and analysed for size using the autocorrelation image-analysis method of Rubin (2004), which, when properly calibrated, has been shown to rapidly yield an accurate measure of mean sediment size (Gallagher et al., 2006).

The underwater video was de-compiled into individual frames, each representing 1/25th second and converted to greyscale. The individual images were filtered for speckle (electrical) noise using a relaxed-median filter (Hamza et al., 1999). Other sources of noise, for example motion blur and non-uniform illumination, were filtered using a complex-valued, log-Gabor wavelet filter described by Kovesi (1999). This algorithm has shown to be particularly efficient for removing non-uniform patches of illumination, especially in underwater imagery (Arnold-Bos et al., 2005). The greyscale image was cropped to the region of interest for sediment transport/bed mobility calculations. A two-dimensional correlation was applied between pixels in consecutive high-resolution greyscale images separated in time by $\delta t = 1/25$ s. This algorithm provided a relative measure of correlation between consecutive frames of a moving bed, and proved useful as a dimensionless 'bed motion' coefficient, Ω:

$$\Omega = 1 \Big/ \frac{\sum_m \sum_n (\alpha)(\beta)}{\sqrt{\left[\sum_m \sum_n (\alpha)^2\right] - \left[\sum_m \sum_n (\beta)^2\right]}} \qquad (1)$$

$$\alpha = I^t_{mn} - \overline{I}^t \quad \beta = I^{t+1}_{mn} - \overline{I}^{t+1}$$

where t is time, m and n are dimensions of image I and the overbar denotes the mean. This yielded a value between 0 and 1, which is very sensitive to changes in 'texture' between consecutive frames, and when other sources of change are removed by filtering, it becomes a sensitive indicator of gross bed mobility. In this way it is a similar process to that of Holland et al. (2001), which tracked image 'texture' to quantify swash flows from video imagery. High values of Ω indicate poorer correlation, therefore most change, and most sediment transport. Remaining differences between frames associated with electrical/optical noise after extensive filtering were minimal (<0.0001). Subsequently, the time series of Ω was re-sampled to 4 Hz to correspond to the hydrodynamic time series.

2.4. Sampling framework

The sampling framework of the experiment was determined by the morphological response of the beachface. Previous field observations at Slapton (Austin, 2005; Austin and

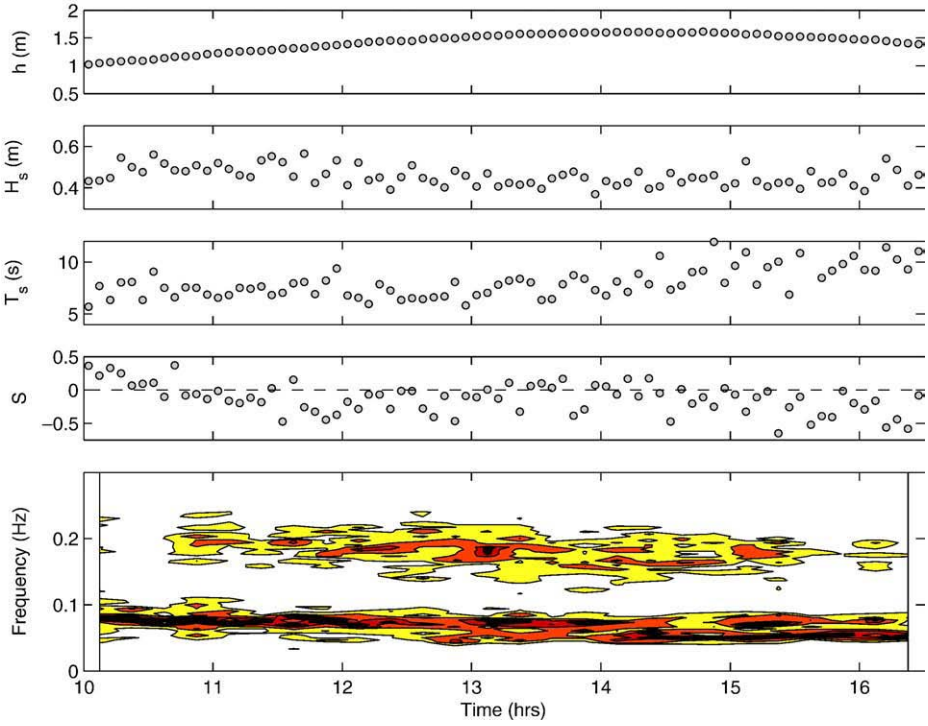

Fig. 4. Hydrodynamic conditions encountered during the field experiment—local water depth h; significant wave height H_s; significant wave period T_s; and wave skewness S. The contour plot in the lower panel represents the temporal evolution of the inshore wave spectrum. The spectra are normalised by their total variance, such that the contour plot shows the change in spectral shape, and not total energy content.

Masselink, 2006) indicated that the step was most active in the hours immediately either side of high water, and was frequently absent around low water, instead replaced by a series of two or more shallower-sided sub-tidal ripple features (similar to those described on Chesil by Hart and Plint (1989), but within closure depth, i.e., not relict features). With one of the aims of the exercise being to monitor step-berm coupling, it was decided to deploy the instruments from mid-tide onwards (~5 h before high water), before the step had formed. Data collection continued during the falling tide, until such a time when beachface morphological change was negligible and the step had been destroyed, become insignificant, or migrated seaward of the rig. Therefore data collection was maximised over the high-tide period when morphological change was greatest and, being higher in the tidal frame, more important to the supply of sediment to the upper beach, thus maintaining the convexity so crucial to the protection of the beach's hinterland.

3. Results

The principal field survey was conducted over a single high tide on 27 September 2005 in the centre of Slapton Sands. During the experiment, the beach had a typical convexo-linear fairweather-type profile, with an intertidal gradient tanβ of 0.23, was composed of moderately coarse and well-sorted sediments with a median size across the active beachface of D_{50}=6 mm and the tide range was 1.5 m.

3.1. Hydrodynamics

Over the period of the field experiment, the water-level h in the region of the step varied by 0.75 m, wave height H_s decreased from 0.6 to 0.5 m and the time series of the spectrally-derived wave period T_s indicates that longer period waves were present during the second half of the survey (Fig. 4). Between 10:00 and 12:00, the wave skewness S, calculated using the method of Elgar and Guza (1985), changes from positive ($S \approx 0.5$) to negative ($S \approx -0.5$). Subsequently, an inflection occurs and S is approximately zero until 15:00 when the waves are negatively skewed (suggesting reflection from the beachface). The evolution of the inshore wave spectra demonstrates that the wave field is composed of 5 s and 12 s waves, with the longer period waves becoming more prominent with time.

The hydrodynamic parameters measured at Rig 2 were averaged over each consecutive 5-min period of the high tide and used to compute the following two morphodynamic indices:

$$\epsilon = \frac{4\pi^2 H_s}{g T_s^2 \tan^2 \beta} \tag{2}$$

$$\xi = \frac{\tan \beta}{\sqrt{H_s / L_s}} \tag{3}$$

where ϵ is the surf scaling parameter (Guza and Inman, 1975) and ξ is a shallow water form of the Iribarren number (Battjes, 1974). L_s is the shallow water wave length, g is gravity and tanβ

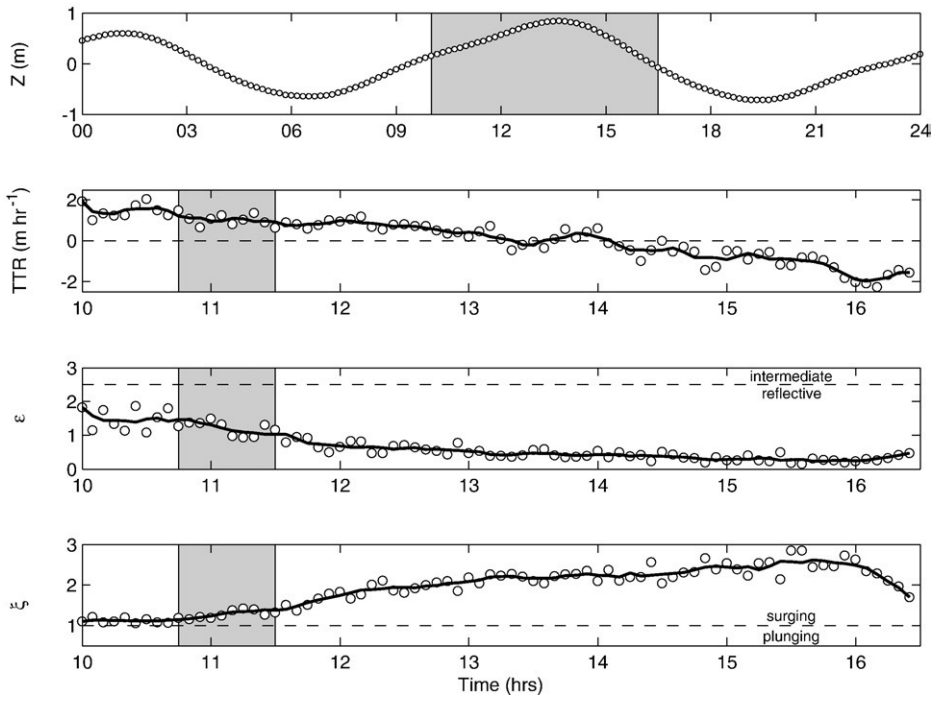

Fig. 5. Time series of tidal elevation and morphodynamic indices for breaker conditions—tidal elevation z (where the shaded region is the experimental period), tidal translation rate TTR, surf scaling parameter ϵ and Iribarren number ξ. The horizontal lines in the middle and lower plots separate morpho-dynamic domains: intermediate versus reflective conditions in the middle panel (Guza and Inman, 1975); and plunging versus surging breakers in the lower panel (Battjes, 1974). The morphodynamic time series have been smoothed using a 5-point moving average indicated by the solid line. The shaded region in the lower three panels indicates the period when ξ initially begins to increase and breaker type becomes predominantly surging.

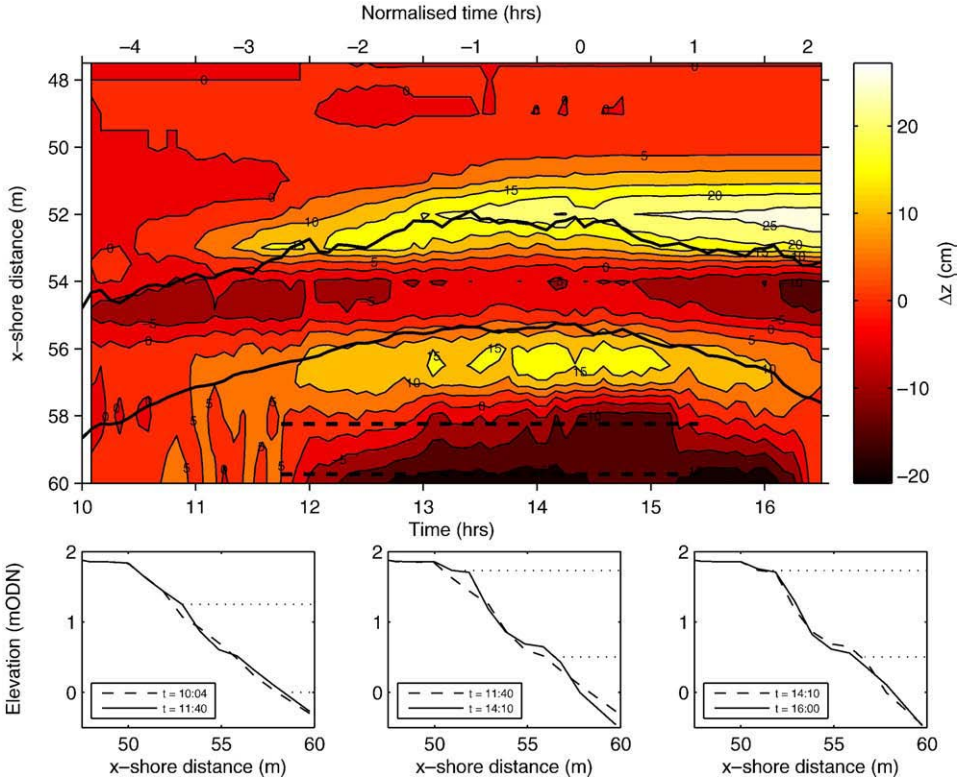

Fig. 6. Morphological evolution of the main transect at cross-shore grid resolution of 0.5 m (upper panel). The shading represents the residual bed-level change relative to the first profile and the contours show elevation change at 5 cm intervals. Temporal profile change during selected periods (lower panels). The thick solid lines in the upper panel represent the $R_{2\%}$ and $R_{80\%}$ run-up limits and the dashed lines the cross-shore position and duration of deployment of the instrument rigs. Time normalised relative to high tide is shown on the upper axis. In the lower panels, the dotted lines indicate the maximum extent of the swash zone during that interval.

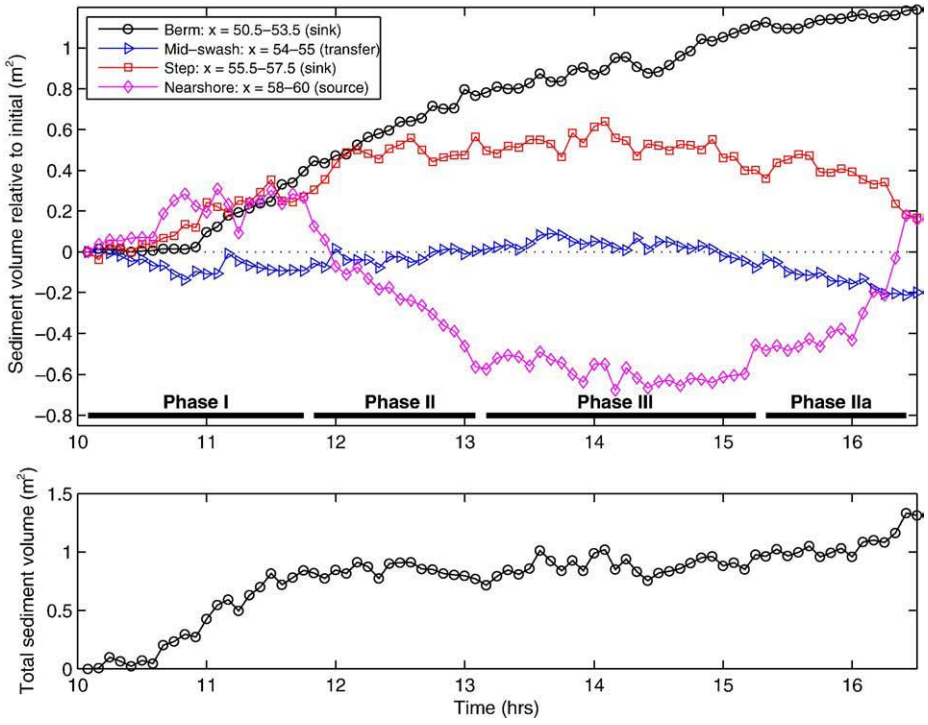

Fig. 7. Volumetric beach change. Upper panel—variation in the sediment volume over the survey period at four cross-shore locations on the beachface. Lower panel—total change in beachface sediment volume during tidal inundation.

is the beach gradient across the 'active' region of the beachface (between the $R_{2\%}$ and $R_{80\%}$ run-up limits). The tidal translation rate TTR was obtained from the run-up data, and calculated as the cross-shore excursion of the $R_{2\%}$ run-up limit between consecutive 5-min periods; as such it integrates fluctuations caused by the tide, incident wave energy and breaker type.

$$\mathrm{TTR} = \frac{\delta x_{R2\%}}{\delta t}. \quad (4)$$

The overall semi-diurnal tidal curve (measured at PT3), TTR, ϵ and ξ are plotted in Fig. 5 and highlight changes in the beach morphodynamics occurring during the tide. The tidal curve is slightly asymmetric, with a more gradual change in depth during the rising tide compared to during the falling tide. During the initial 1.5 h of high tide, wave breaking is close to the plunging/surging transition ($\xi = 1$); wave breaking then moves rapidly into the fully surging regime ($\xi \gg 1.5$) until 16:00, when ξ decreases. The beachface is predicted to be reflective ($\epsilon < 2.5$), but after 11:30 ϵ decreases to $\epsilon \approx 0.5$, indicating strongly reflective conditions, until 16:00 when reflectivity begins to decrease.

3.2. Morphological response

The evolution of the intertidal beach profile along the main transect during the survey period is shown in Fig. 6. Four distinct cross-shore regions can be identified across the beach profile, from seawards: the nearshore ($x = 57.5$ to 60 m); beach step ($x = 55.5$ to 57.5 m); mid swash ($x = 54$ to 55 m); and berm ($x = 50.5$ to 53.5 m). The berm and step appear principally to be accretionary features, whilst the nearshore is erosionary; little change in sediment volume occurs in the mid-swash region. To quantify the morphological response, the changes in sediment volume, relative to the start volume, were computed across each region (Fig. 7—upper panel). Four distinct periods of morphological adjustment can be identified: (1) Phase I is associated with the initial tidal inundation of the beachface and displays moderate volumetric change; (2) Phase II corresponds to the rapid erosion of the nearshore region and strong growth of the step and berm; (3) during Phase III, there is continued berm growth but the lower-beachface is in near-equilibrium with the forcing; and (4) Phase IIa reciprocates Phase II during the ebb tide. During tidal inundation the beachface does not conserve mass; there is a net increase of 1.4 m^2 in sediment volume across each unit metre of beachface (Fig. 7—lower panel). This sediment must either be sourced from the nearshore region or is the result of longshore transport. Grouped variable scatter plots of the step and berm morphological facets plainly differentiate between the two systems (Fig. 8). The coupled step-nearshore–mid-swash systems clearly display hysteresis loops, the distribution of which are strongly related to the phases of morphological change identified in Fig. 7 and hence the tidal translation. In contrast, the berm system displays no hysteresis, and is clearly un-coupled, at least at this time scale, from the nearshore and mid-swash regions.

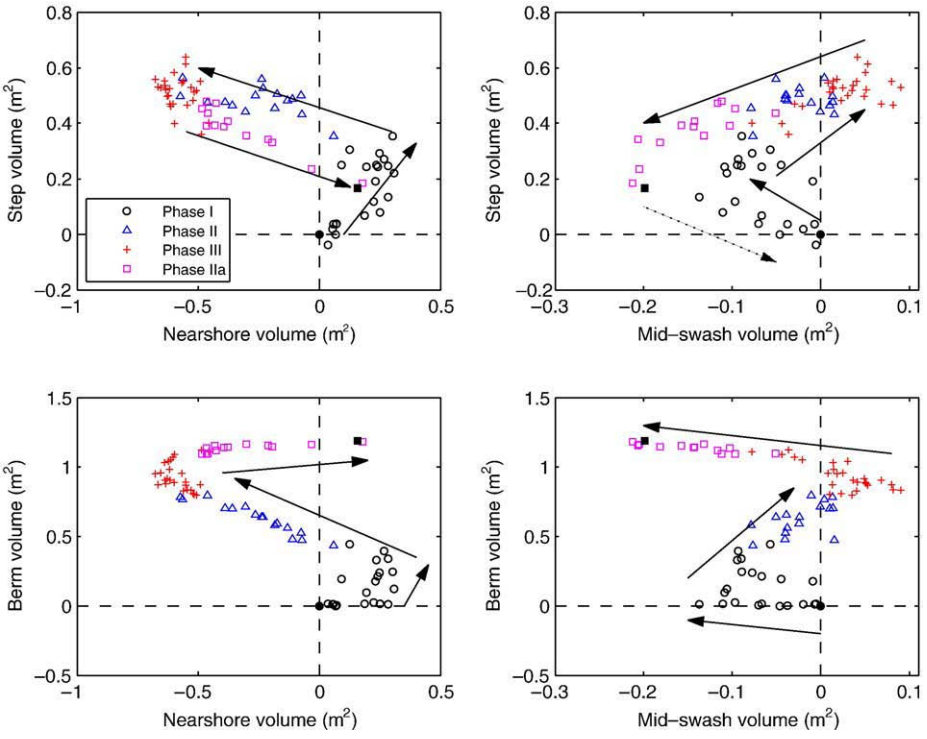

Fig. 8. Grouped variable scatter plots of the different morphological facets. Upper panels—evolution of the beach step compared with the nearshore and mid-swash regions. Lower panels—berm evolution compared with the nearshore and mid swash. The different marker types reflect the phases of morphological change identified in Fig. 7 and the solid circles and squares indicate the start and end points of the sampling period, respectively. Arrows indicate the progression of the morphological change. Sediment volume is measured per unit width of beachface.

3.3. Sedimentology

The following discussion concerns the region of the near-shore where concurrent morphological and sedimentological results are available at sufficient temporal resolution to warrant discussion, namely the region from the step face to mid swash (50–60 m cross-shore distance). Sediment size and morphological change relative to the standard deviation was found to be the most meaningful comparison, and due to the discordant sampling strategy between the morphological and sedimentological record, and the noisy and irregular nature of the sediment size record, only the gross morpho-sedimentary trends could be considered. As a pre-analysis tool the morphological and sediment size data sets were de-constructed using empirical orthogonal functions (EOFs) in order to separate the dominant signals from the fluctuations, about which we could have less certainty. This type of analysis is commonplace in the coastal sciences (e.g. Winant et al., 1975; Aubrey and Ross, 1985; Larson et al., 2003) where the spatio-temporal evolution of a feature such as morphology (e.g., Winant et al., 1975) and grain-size (e.g. Liu and Zarillo, 1989) requires revelation beyond traditional descriptive statistics. It is also beneficial when there are missing data, and where two-dimensional data is sampled with irregular frequency. The eigenfunctions of a data set are ranked according to the proportion of variance explained by that function, and the data can then be reconstructed using only the dominant functions, and the individual components can be considered and compared.

Fig. 9a and b show the original change in morphology and sediment size (relative at each time step to the standard deviation of sediment sizes across space), respectively. The morphological and sediment size data were re-mapped as a 'cleaner' trend with which to draw inference using the number of EOFs required to explain >90% of the variance in the morphology and sedimentology, 2 and 4 EOFs, respectively (Fig. 9c and d). The errors between the original and reconstructed data, calculated as $\Delta R_{\mathrm{EOF}} = \sqrt{\Sigma\left(|y-\hat{y}|^2\right)}$, where y is the original data, and $y\hat{}$ is the reconstructed data, associated with these reconstructions are negligible. The region of foreshore from the berm face to the step crest (50–56 m) became generally coarser throughout the experiment (Fig. 9d), whereas the region just seaward of the step became finer (56–60 m). The main morphological trends are again seen, with the *in-situ* growth of a berm and step. The sedimentological trends are also clearer, with bands of relatively coarse and fine sediments showing some spatio-temporal persistence.

Fig. 10a plots the percentage of explained variance attributable to each EOF. It demonstrates that over 90% of morphological and sedimentological change can be described by two and four EOFs, respectively. It is possible to look for co-variability in the morph-sedimentary signal having first reconstructed the data to show the dominant trends. Overall for the whole beachface, and at the time scale used here, there is little correlation between the morphological and sedimentological signals (Fig. 10b). This is confirmed by the sum of the temporal derivatives of Δz (cm) and ΔD (mm), which display

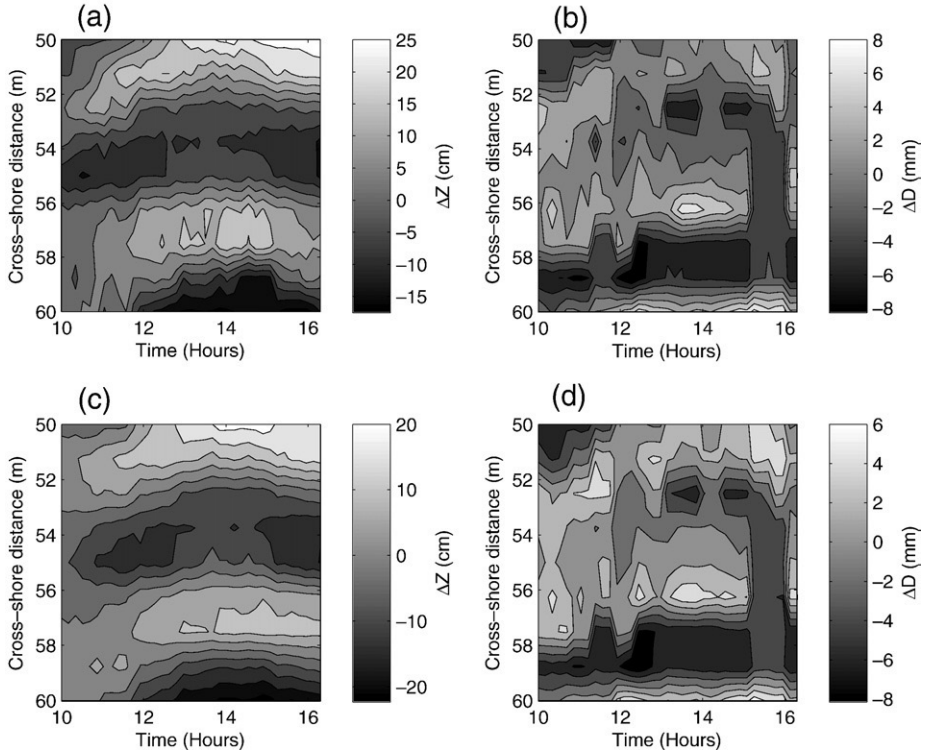

Fig. 9. EOF analysis of morpho-sedimentological trends. (a) Cumulative change in bed elevation relative to initial profile Δz (cm); (b) cumulative change in sediment size relative to the sediment size standard deviation for every cross-shore position over the entire measurement period ΔD (mm); (c) EOF-reconstruction of the morphological data in (a), using the first 2 EOFs, which account for >90% variance; and (d) EOF-reconstruction of the Sedimentological data in (b), using the first 4 EOFs, which account for >90% variance.

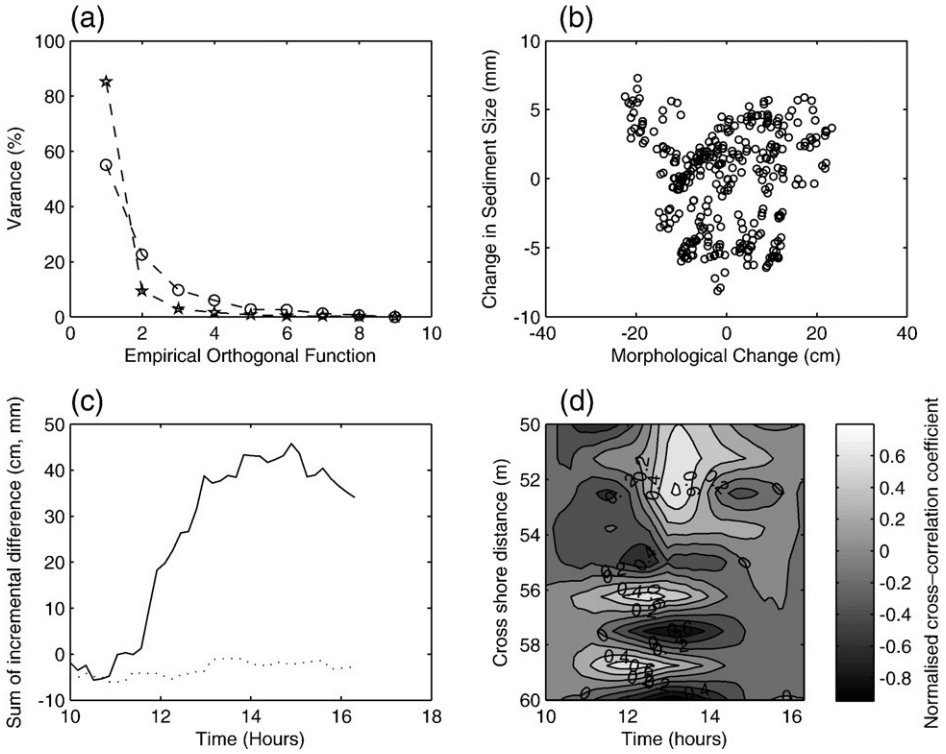

Fig. 10. Morpho-sedimentary dynamics of the nearshore region. (a) Scree plot of percentage explained morphological (pentagons) and sedimentological (circles) variance associated with each EOF; (b) morphological and sedimentological change has an uncorrelated domain of co-variation; (c) the sum of the temporal derivative (solid line) of Δz (cm) and (dotted line) ΔD (mm), relative to starting conditions; and (d) contour plot of morpho-sedimentary cross-correlation (cross-correlation coefficients normalised so that the autocorrelations at zero lag equal unity).

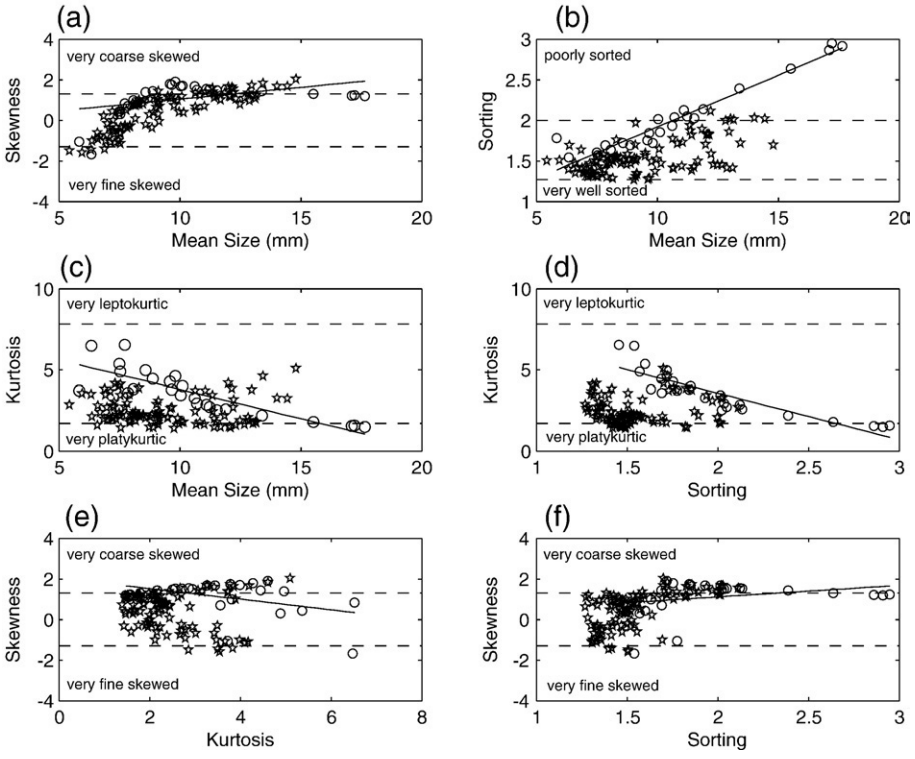

Fig. 11. Sedimentology of the step and foreshore region. Pentagons are mid-swash sediments, and circles are step face sediments. The upper and lower dashed lines delimit regions of classification for each dependent variable shown, based on geometric moments of the distribution. Solid lines show the least squares best fit through the step sediment data.

significantly different trends, relative to the start conditions, through time (Fig. 10c). Cross-correlating the morphological and sedimentological change data demonstrates a maximum correlation ($r=0.6$) across the berm at high tide suggesting that as the berm accretes the sediments become coarser (Fig. 10d). A similar result is observed across the step crest and at the base of the step during the mid-flood tide, but in contrast, the sediment and morphological change are negatively correlated in the nearshore and step face.

Bivariate scatterplots of sedimentary parameters (Fig. 11) reveal some significant correlations in the time series of the step face sediments that are not present in the swash sediments. Relationships were found between sediment parameters only for the step sediments—coarser sediments are more positively skewed (Fig. 11a), more poorly sorted (Fig. 11b), and more platykurtic (Fig. 11c). Perhaps the best parameter to discriminate step and swash sediments is kurtosis—step sediments of a given size are consistently more leptokurtic than swash sediments meaning that, even though overall swash sediments are slightly better sorted, the ratio between the spreads of the tails and centre of the distribution is greater and the step sediments are better sorted in the central part of the distribution.

3.4. Sediment mobility

Sediment transport just seaward of the breaker zone is intermittent, and characterised by periods of relative mobility and relative inactivity. A two-dimensional correlation, as described in Section 2, was applied between 402370 consecutive images, representing ~4.5-hrs of de-compiled video data of the nearshore bed surface at Rig 2. Field observations indicated that the largest transport events occurred at frequencies greater than the incident wave period, suggesting the involvement of wave groups. The role of wave groupiness was investigated by comparing time series of cross-shore current velocity, the wave groupiness envelope and bed motion (Fig. 12). The groupiness envelope was computed by lowpass-filtering the modulus of the cross-shore current record at 0.05 Hz. Visual inspection of the time series indicates that the structure of the groupiness envelope is very similar to, but slightly lagged behind that of the bed motion. The cross-correlation function between the groupiness envelope and the lowpass-filtered bed motion confirms the strong positive correlation, and quantifies the time lag as 5 s. Closer observation of the time series of u and Ω suggests that strong backwashes at the start of the wave group initiate maximum bed mobilisation. The 5 s time lag exists because the maxima of the wave group envelope function is at the centre of the group, and therefore the cross-correlation ignores the effect of first few constituent waves of the group.

Cross-spectral analysis was used to further explore the relationship between Ω and u (Fig. 13). Auto-spectra of the cross-shore current and the bed motion are characterised by a strong peak at 0.08 Hz and a secondary peak at 0.2 Hz for the current, and a peak frequency of 0.03 Hz for the bed motion. These spectral peaks indicate a wave group period of 33 s, and confirm the bi-modal wave field of 12.5 s swell, and 5 s wind waves. There is generally very poor correlation between Ω and u, except at the wave group frequency during Phase I of the

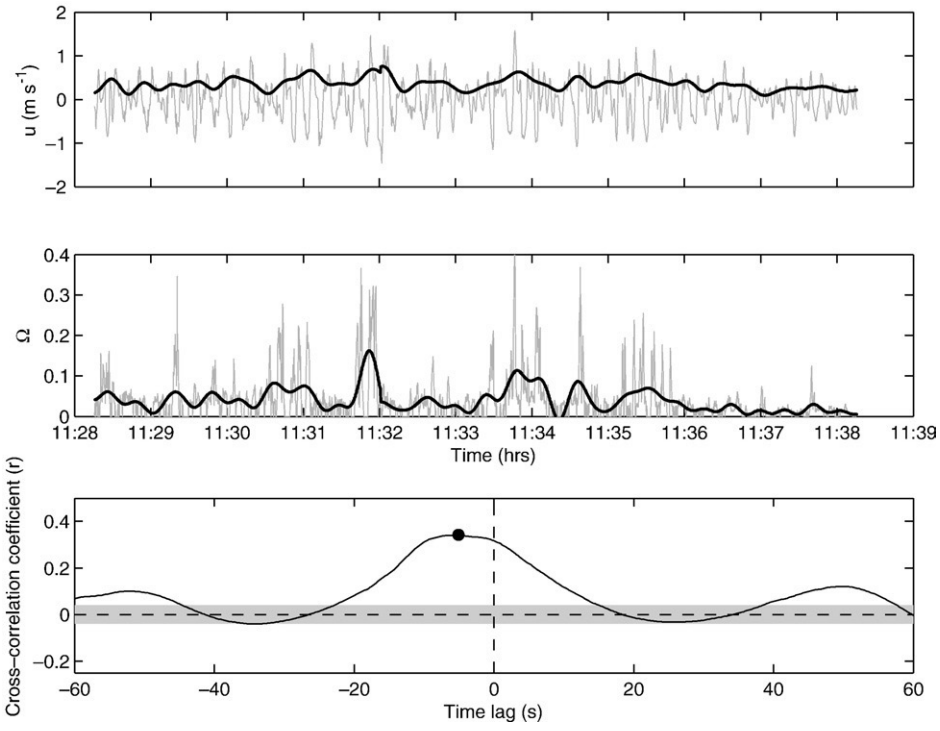

Fig. 12. Time series of (top) cross-shore current velocity u (solid line) and envelope function of u (thick solid line); (centre) non-dimensional bed motion Ω (solid line) and lowpass-filtered Ω (thick solid line); and (bottom) cross-correlation between the groupiness envelope and the lowpass-filtered Ω. The solid circle indicates the maximum correlation coefficient and the shaded region represents the 95% confidence limit calculated as $2/\sqrt{N}$, where N is the number of samples. The cut-off for the lowpass-filter was 0.05 Hz.

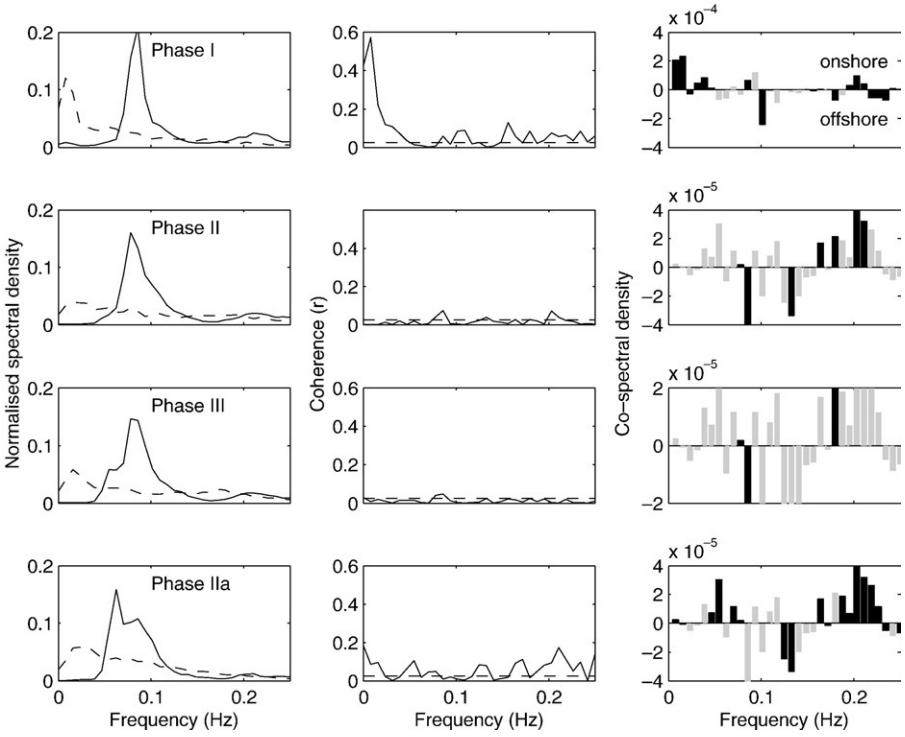

Fig. 13. Spectral analysis of u and Ω during the four previously identified phases of morphological change. Left panels—normalised auto-spectra of u (solid line) and Ω (dashed line); centre panels—coherence spectra (solid line) and 95% confidence limit (dashed line); right panels—co-spectra. Frequencies where u and Ω are significantly coherent are shown in black, grey bars indicate non-significant correlation. The normalised auto-spectra were computed by dividing the individual spectral estimates by the sum of the spectral estimates (i.e., total variance of the time series).

morphological change, and this is further reflected when the co-spectra are calculated between current velocity and sediment motion (Huntley and Hanes, 1987), which are often barely significant over the frequencies of interest. Using Ω as a proxy for sediment transport, the co-spectra quantify the magnitude and direction of the sediment flux at different frequencies in the same way as the co-spectrum between u and the suspended sediment concentration on a sandy beach. During Phase I, maximum bed motion coincides with the onshore phase of the wave-oscillatory currents at the wave group and windwave frequencies; there is some offshore transport at swell frequencies. Progressing into Phases II and III, where significant, transport is onshore due to wind waves and offshore due to swell; transport at the wave group frequencies is largely insignificant. Onshore transport continues at wind wave frequencies throughout Phase IIa with some onshore contribution from the swell.

4. Discussion

The field measurements presented in the present paper describe the morpho-sedimentary evolution of the beach step over a tidal cycle on a macrotidal fine gravel beach. Our results indicate that morphological change at different cross-shore locations across the beachface can be de-coupled, partially due to relaxation time effects, but that these changes may be reflected by corresponding sedimentological changes. We also present the results obtained from a novel method of quantifying bed motion, and hence sediment transport, and demonstrate a link with wave groups.

Referring to the measured morphological change, it is evident from the sediment volumes, that as the tide begins to flood, the beachface initially undergoes a phase of consolidation. This is succeeded by a period of rapid morphological change during the mid-flood when the step and berm develop, followed a quiescent period over the high-tide still-stand. The berm and step then exhibit contrasting morphological behaviour, whereby the berm is consolidated, whilst the step returns to a similar state to that before tidal inundation. However, due to the short temporal scale of the present experiment, it is useful to directly compare our results with those of other experiments for the reason of reproducibility.

Fig. 14 shows the beachface evolution during two other morphological experiments carried out at Slapton using the same methods as above and during similar neap tide moderate- to low-energy conditions (Table 1). The gross morphological changes which occurred across the beachface during the present study are consistent with the other findings, in particular those of Austin and Masselink (2006), where both the spatial distribution and temporal phasing of the step and berm development are in excellent agreement. During the study of Buscombe (in preparation), the magnitude of the morphological changes was significantly smaller due to calm wave conditions, but the trends similar.

During the present study and that of Austin and Masselink (2006), the step and berm were principally accretionary features linked to the tidal stage; however, the step and berm display several dissimilarities that lead to the question of whether they exhibit co-dependent behaviour or are independent features.

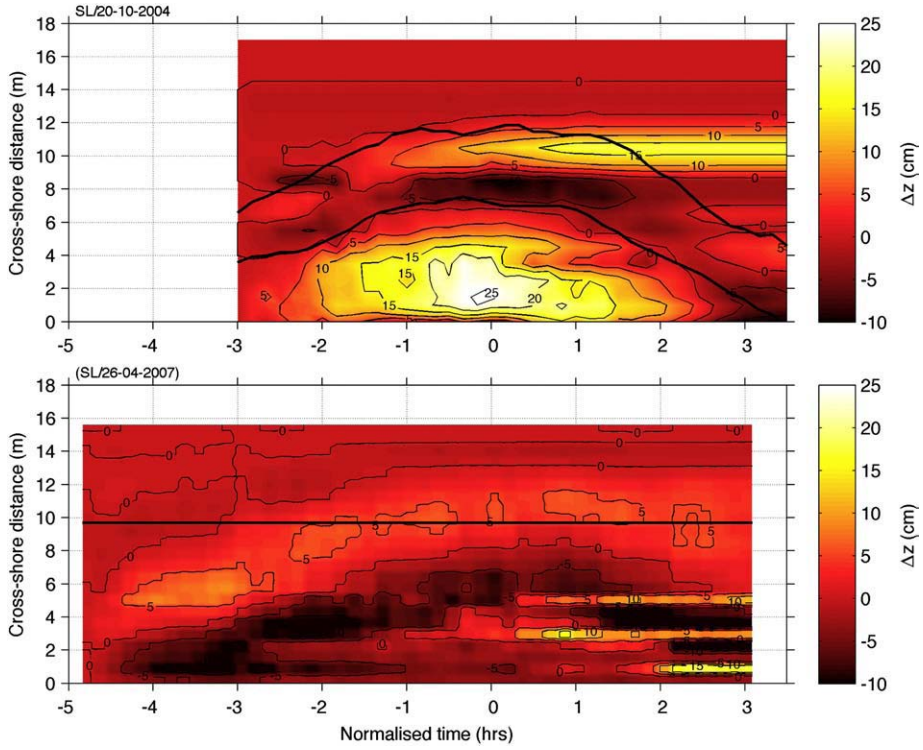

Fig. 14. Morphological evolution during the comparable experiments of Austin and Masselink (2006) and Buscombe (in preparation) at cross-shore grid resolution of 0.5 m. The shading represents the residual bed-level change relative to the first profile and the contours show elevation change at 5 cm intervals. Time has been normalised relative to the time at high tide and the thick lines in the upper and lower panels represent the $R_{2\%}$ and $R_{80\%}$ run-up limits and the maximum run-up limit, respectively.

The step built *in-situ*, with its crest remaining at approximately the same contour throughout the sampling period, whilst in contrast the berm crest migrated landwards by ~1.5 m. The toe of the berm remained at a fixed cross-shore position so the entire berm structure did not move onshore, but rather swash washed sediment over the crest which was re-established landwards. However, during the study of Buscombe (in preparation), the whole structure of the small berm migrated landwards. During the present study, there was a net increase in sediment volume across the beachface, and whilst the volume of sediment eroded from the nearshore and mid swash was roughly balanced by accretion at the step, the volume of material incorporated into the berm did not correspond to the erosion; this material must either have come from seawards of the step or was recycled from the step which was subsequently recharged from offshore. Alternatively, sediment supply to the berm and step was both ample and equal, but differing hydrodynamic or hydraulic forcing caused different patterns of sedimentation. Longshore transport was not considered to provide a significant sediment contribution since previous studies have demonstrated that, at the time scale in question, Slapton is remarkably alongshore uniform (Austin, 2005).

Net berm growth results from swash asymmetry (Duncan, 1964; Eliot and Clarke, 1988), whereas the step forms at the point of convergence between offshore transport in the mid- and lower swash and onshore transport of sediment eroded from the nearshore. Under these conditions, the step is an ephemeral feature with a short relaxation time that forms during the flood phase of the tide and is destroyed during the ebb. Step face sediments are sourced from the nearshore region and transported onshore to converge with sediment sourced from the lower swash which builds up the step crestal region. During the ebb, the crestal region is eroded and its constituent sediment returned to the nearshore. The berm develops coincidentally to the step during the flood, however, it has a relaxation time that is related to the spring–neap cycle and, unlike the step, persists on the beachface because it remains stranded above the shoreline as the tide ebbs; therefore, the berm conserves its sediment over a single high tide whereas the step does not. Consequently there is hysteresis between the coupled mid-swash–step–nearshore region, but not between the un-coupled berm–mid-swash or berm–nearshore regions.

Longshore transport, which primarily occurs in the swash zone of coarse beaches (van Wellen et al., 2001), may be of greater importance to the maintenance of the distinct two-dimensionality found on pure gravel beaches such as Slapton in the longer term. Alongshore transport serves to either supply or remove material to the cross-shore profile of interest, but in such a way as the removal takes place uniformly across the profile. Sherman and Nordstrom

Table 1
Hydrodynamic conditions during the present field experiment and the comparative field studies of Austin and Masselink (2006) and Buscombe (in preparation)

Experiment	H_s (m)	T_s (s)	Tide range (m)
SL/27-09-2005; present	0.46	8	1.5
SL/20-10-2004; Austin and Masselink (2006)	0.5	5	2.2
SL/26-04-2007; Buscombe (in preparation)	0.15	7	1.7

(1985) term this process 'swash grazing', but whereas on sand beaches this leads to scarping, on gravel beaches, because of the strength of individual backwashes under the influence of steeper slopes, it leads to more spatially-uniform sedimentation patterns. Thus, in the short-term, cross-shore transport processes are thought to account for the existence and cross-shore location of secondary morphological features such as the berm and step, but alongshore sediment transport processes may be responsible for the gross sediment supply and thus the slope of the foreshore at longer time scales. Part of the reason for the different relaxation times of the berm and the step may be that alongshore sediment transport processes partially control the amplitude of the berm relative to the foreshore, but not the amplitude of the step (at least not directly). This is because the gradients in alongshore sediment transport may not be sufficiently strong at the breakpoint, given the extent of the forward momentum of the (highly non-linear) waves. Indirectly, however, the volumes contributed or removed by alongshore transport on a given cross-shore stretch of beach may contribute to the supply at the step.

One of the key points of interest during this experiment is why the rate of morphological change suddenly accelerated at 11:30 with the ensuing step formation. Considering the degree of morphological change that occurred across the beachface over the high-tide period, the hydrodynamic conditions remained remarkably consistent. At the initiation of the step, there was no coincident change in H or T_s, or the proportion of low-frequency motions as reported by Ivamy and Kench (2006). The only change observed was in S, from negative to positive, suggesting a switch from offshore to onshore sediment transport if following an energetics approach (Bailard, 1981); however, as Austin and Masselink (2006) demonstrated, the direction of net sediment transport is not correlated to S across the nearshore at Slapton. Of potentially greater significance is the stationarity of the tide. The step is a region of sediment convergence between offshore transport in the lower swash and onshore advection under the breaking waves. During periods of rapid tidal translation, there is insufficient time for a step to form at the convergence point, which simply migrates with the breakpoint; however, once the TTR decreases approaching high tide, a point is reached whereby there is sufficient time (stationarity) to trigger step formation. Subsequently, positive feedback takes over and the reduction in water depth and increased beachface steepness forces wave breaking over the step, further increasing its height. Any backwash vortex which may be present will also be amplified by the positive feedback and will induce further sedimentation as described by Larson and Sunamura (1993). The positive feedback is clearly illustrated by the rapid increase in the Irribarren number as waves are forced from breaking at the transition of plunging–surging to being firmly within the surging regime. It is probable that there is a linear relationship between the wave and step height (Hughes and Cowell, 1987), with the step adjusting to reach an equilibrium height that is proportional to that of the waves. During the falling tide, once the change in h and TTR increases above a certain limit, the seaward migration of the breakpoint breaks the cycle of positive feedback with the step, which then begins to be eroded by the backwash and smeared across the beachface. It is interesting to note that the step appears to be destroyed more rapidly during the falling tide than it is formed during the rising tide. This may be related to the asymmetry in $\delta h/\delta t$ observed in the semi-diurnal tidal curve and may also provide an explanation as to why the step is absent at low tide (Fig. 5).

Changes in the sedimentology, unlike those of nearshore volumetric change, display no significant hysteresis; however, there are some interesting trends in the sediment size data which can be attributed to associated morphologies. The sediments are not as negatively skewed as is common with beach sediments (Masselink and Hughes, 2003), indicating the presence of a more mobile coarse fraction than is common on sand beaches, and corroborated by the general coarseness of the step and berm. The coarsening of the upper berm is consistent with observations from earlier work (e.g. Duncan, 1964; Masselink and Li, 2001), and whilst the four distinct phases of morphological change are not clearly reflected in the sedimentary signal, temporal changes in the sedimentology can be related to the morphological response across regions of the beachface. At the berm, step crest and just seaward of the step, accretion (erosion) is linked to coarsening (fining) of the sediments. Conversely, across the step face and part of the nearshore, the negative correlation between sediments and morphology indicates divergent behaviour; accretion is associated with fining and erosion with coarsening. The coarsening of the step sediments over high tide can be attributed to the preferential removal of fine sediments, seawards to the base of the step and landwards to the mid swash. In contrast to Strahler (1966), who suggested that the coarse sediments accumulated at the step since they could more easily be transported over the finer sediments either side of the step, these findings indicate that the coarse sediments at the step constitute a lag deposit. Subsequently, during the falling tide, the retreating swash smears the fine mid-swash sediments over the lower beachface. These findings contradict those of Masselink et al. (2007), that temporal changes in sedimentology were unrelated to the morphological response, and qualitatively support the use of sediment trend models such as McLaren and Bowles (1985), or perhaps more correctly Gao and Collins (1992) considering the oscillatory nature of the transport processes. However, whether or not such models would be suited in the swash where strong gradients in sediment transport direction do not exist, remains to be seen (Masselink et al., in press).

The inability to discern more obvious trends in step and beachface sedimentology is probably related to shortcomings in the sediment sampling strategy; most noticeably, much higher resolution sampling of the sediments is required. Sediment size distributions are found to vary on a time-scale comparable to the hydrodynamic forcing (wave time-scale), not the morphological changes; improper sampling of the sedimentary signal may cause high-frequency components to be aliased with genuine low-frequency ones. Furthermore, only the top layer of the bed was sampled across the sub-aerial beachface and this may not have been representative of the active layer of the beachface as a whole since the presence of vertical variations in grain-size in beach sediment is well known in the form of laminae (Emery, 1978) and dual sedimentation units (Duncan, 1964). However,

the assertion that the step and berm are not morphodynamically co-dependent is mirrored by the surficial sedimentary record.

This study has attempted to measure instantaneous cross-shore sediment transport on a gravel beach using a novel video remote sensing method. Whilst suspended sediment transport can be measured with relative ease on sandy beaches with optical and acoustic backscatter sensors, the quantification of the bedload and sheet flow modes of transport that prevail on gravel beaches is a much greater challenge. The implementation of the video-based bed monitoring system and the non-dimensional bed motion parameter Ω provides a means to quantify the sediment transport through the change in bed texture. The results clearly demonstrate periodic transport due to the elevated flow velocities under wave group crests (e.g. Hanes, 1991; Huntley and Hanes, 1987), but the issue of similar magnitude velocity events causing differing bed responses causes problems when interpreting sediment fluxes. For example, in Fig. 12, the flow velocity at 11:28–11:29 is comparable to that at 11:36–11:37, but Ω is twice as large during the former. The net result of this observation is poor coherence between Ω and u when the spectra are computed. On the whole, sediment transport is onshore at wind wave and wave group frequencies, but that due to swell is highly variable. This accounts for the net onshore-directed morphological change across the upper beachface (i.e. the conservation of berm sediments), but the lower beachface was approximately in equilibrium with the prevailing hydrodynamic conditions so this onshore transport must somehow be compensated by offshore transport. It is tentatively suggested that this occurs during the falling tide due to three mechanisms: (1) the tail end of the backwash increasingly acting upon the step crest and avalanching sediment down the step face; (2) the return of the wave breaker type towards the plunging–surging transition; and (3) the drainage of groundwater from the beachface during the falling tide (Austin and Masselink, 2006).

The sediment transport events indicated by Ω may not be linearly proportional to the instantaneous volumetric sediment flux and hence may be the reason why there are many occasions where the bed motion induced by two similar velocity events is very different. There are several possible mechanical explanations for the differing bed responses to velocity events of similar magnitude, but changes in bed roughness due to the wide variation of grain sizes may be the main cause. It was frequently observed that changes in sediment size and distribution could occur on a wave-by-wave basis. It is therefore conceivable that an instantaneous change in the textural properties of the bed during one transport event may cause either positive or negative feedback upon the system by changing sediment transport thresholds. For example, if one transport event results in sediment coarsening through the removal of fines, this will cause an increase in bed roughness through greater protrusion of the remaining larger grains into the boundary layer. This has at least three possible repercussions: (1) an increase in bed shear stress and turbulence leading to greater sediment mobility; (2) preferential transport of the largest grains due to their protrusion into the boundary layer; or (3) reduced mobility due to the larger entrainment thresholds of the bigger grains. Consequently, the following velocity event of similar magnitude may result in very different rates of bed motion. Therefore a better correlation may be obtained between Ω and a shear stress parameter incorporating a variable bed roughness term, i.e. a Shields parameter containing a time-variant friction factor; however, this requires a priori or antecedent knowledge of the instantaneous grain size/distribution.

5. Conclusions

Measurements of temporal and spatial changes in morphology and sediment dynamics across the inter-tidal zone have been acquired from a macrotidal gravel beach. Incident frequency wave heights remained constant throughout the deployment; however, significant morpho-sedimentary change occurred where an ephemeral beach step evolved under the breakpoint and a berm formed in the upper swash.

Morphologically speaking, the step and berm develop as independent features. The berm forms due to onshore swash asymmetry and has a relaxation time linked to the phase of the spring–neap tidal cycle, whilst the step is the result of sediment convergence at the break point with a shorter relaxation time linked to the semi-diurnal tide. Some initial perturbation triggered the initiation of the step, probably the reduction of the tidal translation rate (TTR) or changing water depth, which caused the point of sediment convergence to become stationary towards high tide. Positive feedback then acted to reinforce the morphological change, indicated by a switch in wave breaker type from plunging–surging to fully surging. The step remained in place until the falling tide, whereby the increasing TTR and reduction in water depth caused the seaward migration of the breakpoint and subsequent smearing and removal of the step.

The beachface is a closed sedimentary unit in the short-term, but the beach step can be differentiated from the berm using sedimentary moments. Distinct phases of morphological change are not clearly evident in the sedimentary signal, however, temporal changes in the sedimentology at several locations on the beachface are related to the morphological response. At the berm and step crest, accretion is associated with sediment coarsening, whereas seaward of the step, accretion is linked to sediment fining. A lag deposit of coarse sediments persists at the step as a divergence of fines occurs; these are preferentially removed to the swash zone and nearshore. Despite the location of the step at the locus of wave breaking, it has relatively stable sedimentology, remaining characteristically coarser and more leptokurtic than the swash zone. The inability to discern more obvious trends in sedimentology is related to the sampling strategy; sediment size distributions were observed to vary on a wave rather than morphological change time scale so much higher resolution sediment sampling is therefore required.

Periodic bed motion (Ω) was observed at sub-incident frequencies (~35 s) in response to wave groups. Co-spectral analysis between Ω and the cross-shore flow velocity suggests that sediment transport is onshore at wind wave and wave groups frequencies, but highly variable at swell frequencies. However, motion of the nearshore bed is a non-linear function of flow velocity magnitude or direction, and it is likely that

wave–frequency variations in bed roughness cause rapid changes in sediment transport thresholds. This leads to the suggestion of a time-variant friction factor derived from remotely-sensed high-resolution sedimentary sampling.

Acknowledgements

We would like to thank Gerd Masselink, Tamsin Watt, Jon Tinker, George Graham and Ben Allured for their assistance in the field and the Department of Geography, Loughborough University for the loan of the ADV current meters. This work was funded by a post-graduate research grant awarded to MJA by the British Geomorphological Research Group and a departmental studentship awarded to DB by the Faculty of Social Science and Business, University of Plymouth. The authors would also like to thank Gerd Masselink and two anonymous reviewers for their suggestions.

References

Arnold-Bos, A., Malkasse, J.P., Kervern, G., 2005. A pre-processing framework for automatic underwater image denoising. European Conference on Propagation and Systems '05. ECPS, Brest, France.

Aubrey, D.G., Ross, R.M., 1985. The quantitative description of beach cycles. Mar. Geol. 69, 155–170.

Austin, M.J., , 2005. Swash, groundwater and sediment transport processes on a gravel beach. Ph.D. thesis, Department of Geography, Loughborough University, UK.

Austin, M.J., Masselink, G., 2006. Observations of morphological change and sediment transport on a steep gravel beach. Mar. Geol. 229, 59–77.

Austin, M.J., Masselink, G., O'Hare, T., Russell, P.E., 2007. Relaxation time effects of wave ripples on tidal beaches. Geophys. Res. Lett. 34 (L16606). doi:10.1029/2007GL030696.

Bagnold, R.A., 1940. Beach formation by waves: some model experiments in a wave tank. Journal of the Intitute of Civil Engineering Paper 5237, pp. 27–53.

Bailard, J.A., 1981. An energetics total load sediment transport model for a plane sloping beach. J. Geophys. Res. 86, 10938–10954.

Battjes, J.A., 1974. Surf similarity. Proceedings 14th International Conference on Coastal Engineering. ASCE, pp. 466–480.

Bauer, O., Allen, J., 1995. Beach steps: an evolutionary perspective. Mar. Geol. 123, 143–166.

Buscombe, D., Masselink, G., 2006. Concepts in gravel beach dynamics. Earth Sci. Rev. 79, 33–52.

Buscombe, D., in preparation. Morphodynamics, sedimentation and sediment dynamics of a gravel beach. Ph.D. thesis, University of Plymouth.

Davis, R.A., 1985. Beach and nearshore zone. In: Davis, R.A. (Ed.), Coastal Sedimentary Environments. Springer, New York, p. 50.

Dhyr-Nielsen, M., Sorensen, T., 1970. Sand transport phenomena on coasts with bars. Proceedings of the 12th International Conference on Coastal Engineering. ASCE, pp. 855–866.

Duncan, J.R., 1964. The effects of water table and tide cycle on swash–backwash sediment distribution and beach profile development. Mar. Geol. 2 (3), 186–197.

Elgar, S., Guza, R.T., 1985. Observations of bispectra of shoaling surface gravity waves. J. Fluid Mech. 161, 425–448.

Eliot, I.G., Clarke, D.J., 1988. Semi-diurnal variation in beachface aggredation and degradation. Mar. Geol. 79, 1–22.

Emery, K.O., 1978. Grain-size in laminae of beach sand. J. Sediment. Petrol. 48, 1203–1212.

Gallagher, E., MacMahan, J., Russell, P.E., Masselink, G., Auger, N., 2006. Grain size from digital images and morphological variability. Proceedings 30th International Conference on Coastal Engineering. ASCE, San Diego.

Gao, S., Collins, M., 1992. Net sediment transport patterns inferred from grain-size trends, based upon definition of transport vectors. Sediment. Geol. 81 (47–60).

Guillen, J., Palanques, A., 1996. Short- and medium-term grain size changes in deltaic beaches (Ebro Delta, NW Mediterranean). Sediment. Geol. 101, 55–67.

Guza, R.T., Inman, D.L., 1975. Edge waves and beach cusps. J. Geophys. Res. 80, 2997–3012.

Hails, J.R., 1975. Offshore morphology and sediment distribution, Start Bay. Philos. Trans. R. Soc. Lond., A 279, 221–228.

Hamza, A.B., Luque-Escamilla, P.L., Aroza, J.M., Roldan, R.R., 1999. Removing noise and preserving details with relaxed median filters. J. Math. Imaging Vis. 11, 161–177.

Hanes, D.M., 1991. Suspension of sand due to wave groups. J. Geophys. Res. 96, 8911–8915.

Hart, B.S., Plint, A.G., 1989. Gravelly shoreface deposits: a comparison of modern and ancient facies sequences. Sedimentology 36 (4), 551–557.

Hoefel, F., Elgar, S., 2003. Wave-induced sediment transport and sandbar migration. Science 299, 1885–1887.

Holland, K.T., Puleo, J.A., Kooney, T.N., 2001. Quantification of swash flows using video-based particle image velocimetry. Coast. Eng. 44, 65–77.

Hughes, M., Cowell, P., 1987. Adjustment of reflective beaches to waves. J. Coast. Res. 3 (2), 153–167.

Huntley, D.A., Hanes, D.M., 1987. Direct measurement of suspended sediment transport. Coastal Sediments '87. ASCE, pp. 723–737.

Inman, D.L., 1953. Areal and seasonal variations in beach and nearshore sediments at La Jolla, California. Tech. Rep., vol. 39. U.S. Army Corps of Engineering Beach Erosion Technical Board Memo, p. 134.

Ivamy, M.C., Kench, P.S., 2006. Hydrodynamics and morphological adjustment of a mixed sand and gravel beach, Torere, Bay of Plenty, New Zealand. Mar. Geol. 228 (1–4), 137–152.

Kamphuis, J.W., Moir, J.R., 1977. Mean diameter distribution of sediment sizes before and after artificial beach nourishment. Proceedings Coastal Sediments '77. ASCE, New York, p. 569.

Kemp, P.H., 1975. Wave asymmetry in the nearshore zone and breaker area. In: Hails, J., Carr, A. (Eds.), Nearshore Sediment Dynamics and Sedimentation. Wiley, London, pp. 47–67.

Kovesi, P., 1999. Phase preserving denoising of images. The Australian Pattern Recognition Society Conference: DICTA'99. Perth, WA, pp. 212–217.

Krumbein, W.C., 1938. Local areal variations of beach sands. Geol. Soc. Amer. Bull. 49, 653–658.

Kulkarni, C., Levoy, F., Montfort, O., Miles, J.R., 2004. Morphological variations of a mixed sediment beachface (Teignmouth, UK). Cont. Shelf Res. 24, 1203–1218.

Larson, M., Sunamura, T., 1993. Laboratory experiment on flow characteristics at a beach step. J. Sediment. Petrol. 63, 495–500.

Larson, M., Capobianco, M., Jansen, H., Rozynski, G., Southgate, H., Stive, M., Wijnberg, K.M., Hulscher, S., 2003. Analysis and modelling of field data on coastal morphological evolution over yearly and decadal time scales. Part 1: background and linear techniques. J. Coast. Res. 19, 760–775.

Liu, J.T., Zarillo, G.A., 1989. Simulation of grain-size abundances on a barred upper shoreface. Mar. Geol. 109, 237–251.

Losada, M.A., Medina, R., Vidal, C., Losada, I.J., 1992. Temporal and spatial cross-shore distributions of sediment at 'El Puntal' spit, Santander, Spain. Proceedings 23rd International Conference on Coastal Engineering. ASCE, New York, pp. 2251–2264.

Masselink, G., Hughes, M.G., 2003. Introduction to coastal processes and geomorphology. Arnold, London.

Masselink, G., Li, L., 2001. The role of swash infiltration in determining the beachface gradient: a numerical study. Mar. Geol. 176, 139–156.

Masselink, G., Auger, N., Russell, P.E., O'Hare, T., 2007. Short-term morphological change and sediment dynamics in the intertidal zone of a macrotidal beach. Sedimentology 54 (1), 39–54.

Masselink, G., Buscombe, D., Austin, M.J., O'Hare, T., Russell, P.E., in press. Sediment trend models fail to reproduce small-scale sediment transport patterns on an intertidal beach. Sedimentology. doi:10.1111/j.1365-3091.2007.00917.x.

Matsunaga, N., Honji, H., 1980. The backwash vortex. J. Fluid Mech. 99 (4), 813–815.

Matsunaga, N., Honji, H., 1983. The steady and unsteady backwash vortices. J. Fluid Mech. 135, 189–197.

McLaren, P., Bowles, D., 1985. The effects of sediment transport on grain-size distributions. J. Sediment. Petrol. 55, 457–470.

Medina, R., Losada, M.A., Losada, I.J., Vidal, C., 1994. Temporal and spatial relationship between sediment grain size and beach profile. Mar. Geol. 118, 195–206.

Miller, R.L., Zeigler, J.M., 1958. A model relating dynamics and sediment pattern in equilibrium in the region of shoaling waves, breaker zone, and foreshore. J. Geol. 66, 417–441.

Morey, C.R., 1976. The natural history of Slapton Ley Nature Reserve XII. The morphology and history of the lake basins. Field Stud. 4, 353–368.

Nordstrom, K.F., Jackson, N., 1990. Migration of swash zone, step and microtopographic features during tidal cycles on an estuarine beach, Delaware Bay, New Jersey, USA. Mar. Geol. 92, 147–154.

Roelvink, J.A., Stive, M.J.F., 1989. Bar-generating cross-shore flow mechanisms on a beach. J. Geophys. Res. 94 (C4), 4785–4800.

Rubin, D.M., Topping, D.J., 2001. Quantifying the relative importance of flow regulation and grain size resolution of suspended sediment transport α and tracking changes in grain size of bed sediment β. Water Resour. Res. 37, 133–146.

Rubin, D.M., 2004. A simple autocorrelation algorithm for determining grain size from digital images of sediment. J. Sediment. Res. 74, 160–165.

Sallenger, A.H., Richmond, B.M., 1984. High-frequency sediment level oscillations in the swash zone. Mar. Geol. 60, 155–164.

Sherman, D.J., Nordstrom, K.F., 1985. Beach scarps. Z. Geomorphol. 29, 139–152.

Sherman, D.J., Orford, J.D., Carter, R.W.G., 1993. Development of cusp-related, gravel size and shape facies at Malin Head, Ireland. Sedimentology 40, 1139–1152.

Strahler, A.N., 1966. Tidal cycle of changes in an equilibrium beach Sandy Hook, New Jersey. J Geol. 74 (3), 247–267.

Takeda, I., Sunamura, T., 1983. A wave flume experiment of beach steps. Annu. Rep. Inst. Geosci., Univ. Tsukuba 9, 45–48.

Tolman, H.L., 1994. Wind waves and movable-bed bottom friction. J. Phys. Oceanogr. 24, 994–1009.

van Wellen, E., Baldock, T.E., Chadwick, A.J., Simmonds, D.S., 2001. STRAND — a model for longshore sediment transport in the swash zone. In: Edge, B.L. (Ed.), Coastal Engineering 2000. ASCE, Reston, Virginia, pp. 3139–3150.

Winant, C.D., Inman, D.L., Nordstrom, C.E., 1975. Description of seasonal beach changes using empirical eigenfunctions. J. Geophys. Res. 80, 1979–1986.